JOURNAL OF SOLID STATE CHEMISTRY 76, 260–265 (1988)

3.1 GeV-Xenon Ion Latent Tracks in $Bi_2Fe_4O_9$: High-Resolution Electron Microscope Observations*

D. GROULT,† M. HERVIEU, N. NGUYEN, AND B. RAVEAU

Laboratoire de Cristallographie et Sciences des Matériaux, ISMRa, Boulevard du Maréchal Juin, 14032 Caen Cedex, France

Received July 15, 1987; in revised form October 30, 1987

Latent tracks of 3.1 GeV-Xe ions have been visualized by high-resolution electron microscopy in ferrite $Bi_2Fe_4O_9$. The track diameter is larger than in similarly irradiated yttrium iron garnet and barium iron hexaferrite showing the influence of the atomic density and structure in the response of solid to ion impact. Unlike $Y_3Fe_5O_{12}$ and $BaFe_{12}O_{19}$, in $Bi_2Fe_4O_9$ Xenon-latent tracks appear, in a plane normal to the ion beam, as circular areas of nearly amorphous matter without any transition zone between the paramagnetic core of the nuclear track and the surrounding undistorted lattice.

Introduction

Track formation is a fairly general phenomenon observed in dielectric materials irradiated by sufficiently energetic charged particles. It has been extensively studied in numerous micas, silicates, and plastics and discussed in terms of ionization process. The still best accepted theory for track creation mechanism is the ion explosion spike model of Fleischer *et al.* (*1, 2*), according to which tracks are highly disordered regions arising from transient positively charged regions created by electronic stopping.

The model has thus been used by Hansen *et al.* (*3, 4*) to explain magnetic and physical changes induced by xenon and uranium ions of 185 and 333 MeV per ion, respectively, in epitaxial iron garnet films.

Suggested from indirect measurements mainly based on the etching behavior of the latent track, the model did not display any information about the actual microscopic structure of the damage zone. To understand the mechanism of the track formation, transmission electron microscopy (TEM) and more particularly high-resolution electron microscopy (HREM) should be very useful and have in fact been applied to the problem, for instance, to characterize the fission tracks in zircon (*5*).

However, the use of high-resolution imagery presupposes that the latent tracks are sufficiently stable to be observed under the electron beam. Fission fragment tracks were thus visualized in natural micas including biotite, phlogopite, and muscovite (*6–8*); but, in numerous cases, the tracks faded from view, even under low electron beam currents, therefore preventing any HREM investigation. On the contrary magnetic oxides show extreme track stability as it has been reported elsewhere for yttrium

* Experiment performed at the National Laboratory GANIL with the collaboration of CIRIL.

† To whom all correspondence should be addressed.

0022-4596/88 $3.00

iron garnet and barium iron hexaferrite (*9–11*). Recently a study of the damage induced by heavy ion irradiation was undertaken (*12*) in the mixed framework bismuth ferrite $Bi_2Fe_4O_9$ (*13*) whose structure, like those of garnets and barium hexaferrite, involves FeO_6 octahedra and FeO_4 tetrahedra, but exhibits a lower packing density. During this investigation nuclear tracks were observed. The present paper, which corresponds to the second part of this work, deals with the HREM study of 3.1 GeV-xenon tracks in this compound and with an attempt to explain their formation.

Experimental Procedure

The irradiations were carried out at the heavy ion accelerator GANIL in the 77 K irradiation facility of CIRIL as previously described (*14*) with xenon ion beam having an energy per nucleon of 24 MeV, i.e., 3.1 GeV per ion.

The samples investigated during this study correspond to the electronic stopping zone of the incident particles and a fluence close to 10^{12} Xe · cm^{-2}. Thin flakes suitable for HREM observations were obtained from the irradiated samples by splitting in liquid nitrogen to avoid any plastic deformation. After being dispersed in *n*-butanol, numerous fragments were then collected on copper supported holey carbon films. Lattice images representing all stages of lattice destruction due to radiation damage have been visualized using a JEOL 200 CX electron microscope fitted with a double tilt top-entry goniometer (∓10°). The spherical aberration of the objective lens was 0.8 mm and the beam divergence was about 1×10^{-3} rad.

Results and Discussion

Despite a strong overlapping of the tracks, the HREM micrographs taken with the electron beam parallel to the Xe ion beam clearly illustrate the perfect circular shape of the latent tracks. Two examples are given in Figs. 1 and 2. The former corresponds to a portion with a low density of tracks; the zone axis is [1$\bar{1}$3]. The latter relates to a slightly higher density with a more important overlapping of the tracks; the zone axis is [120].

In both cases, it is worth pointing out that the remaining crystalline matrix is neither disturbed nor strained, leading to a particularly abrupt interphase region between the nearly amorphous track volume and the undistorted surrounding lattice. Such a feature has been emphasized in Fig. 3 which is an enlargement of Fig. 2. A track diameter of 120 ∓10 Å can be measured with a good accuracy in fair agreement with the value obtained from Mössbauer spectra (*12*). The microstructural aspect of the track area is thus strongly different from that seen in Ba $Fe_{12}O_{19}$ specimens (*10–15*) for which a dark contrast correlated with the strain field, probably induced by interstitial atoms, has been clearly observed. It develops around a circular area inside which the structure is destroyed giving no image of regular lattice. According to the ion explosion spike model, this is compatible with the energy

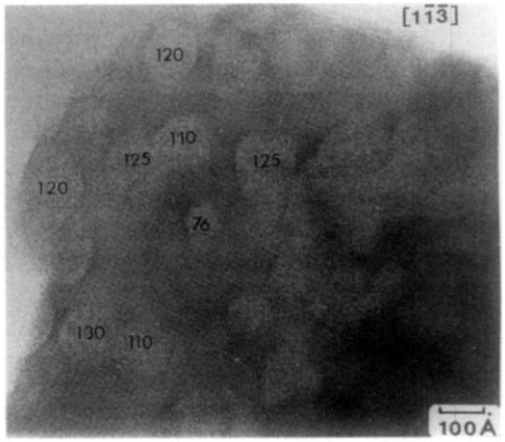

FIG. 1. High-resolution image of 3.1 GeV-Xe latent tracks in $Bi_2Fe_4O_9$; the zone axis is [1$\bar{1}$3].

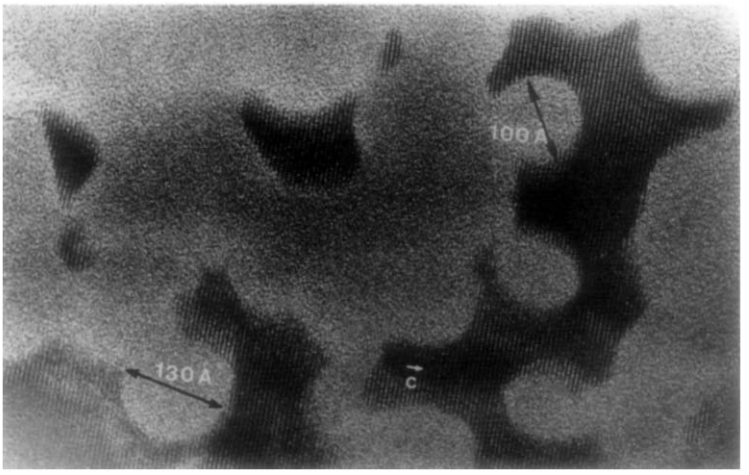

FIG. 2. High-resolution image of latent tracks viewed in a plane normal to the ion beam and showing the sharp boundary between the crystalline and the amorphous parts of the matrix; the zone axis is [120].

lost by ionization process converted into atomic motion and subsequent disorder.

Similar results have also been obtained for $Y_3Fe_5O_{12}$ samples irradiated by Mo and Xe ion beams at 2.3 and 3.1 GeV, respectively (*16*). In the latter case, the direct measurement of the track radius from HREM for several values of the electronic stopping power (dE/dX) reveals a larger cylindrical volume than that deduced from indirect measurements, including vibrating sample magnetometry (VSM), Mössbauer spectroscopy (*17, 18*), and channelling Rutherford back-scattering (RBS) (*16*).

Taking into account previous results reported by Hansen *et al.* (*3*) for thin film of yttrium iron garnet, it can be postulated that the latent track, in that material, consisted of three concentric regions:

(i) a paramagnetic and amorphous core displayed by both VSM and RBS;

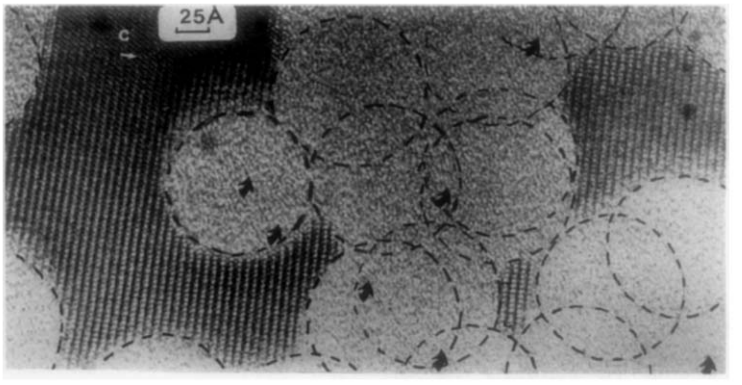

FIG. 3. Enlargement of an area of Fig. 2 and schematic drawing of the tracks: small crystalline islands 20 Å wide can be seen between amorphous parts coming from the overlapping of the tracks.

(ii) a distorted and strained outer shell deduced from HREM, and

(iii) a third zone of crystalline matter, but exhibiting a magnetic hyperfine field *Hf* parallel to the induced strain, i.e., parallel to the ion track as shown from Mössbauer spectra (*18*).

The radius of the cylinder which includes such an *Hf* oriented zone is thus twice that of the paramagnetic core.

In contrast, the structure of the latent track in $Bi_2Fe_4O_9$ is that of a paramagnetic, nearly amorphous cylinder created from the crystalline matter by the incoming ion, without any transition region with the undistorted lattice so that no induced lateral compressive stress seems to occur (*9*).

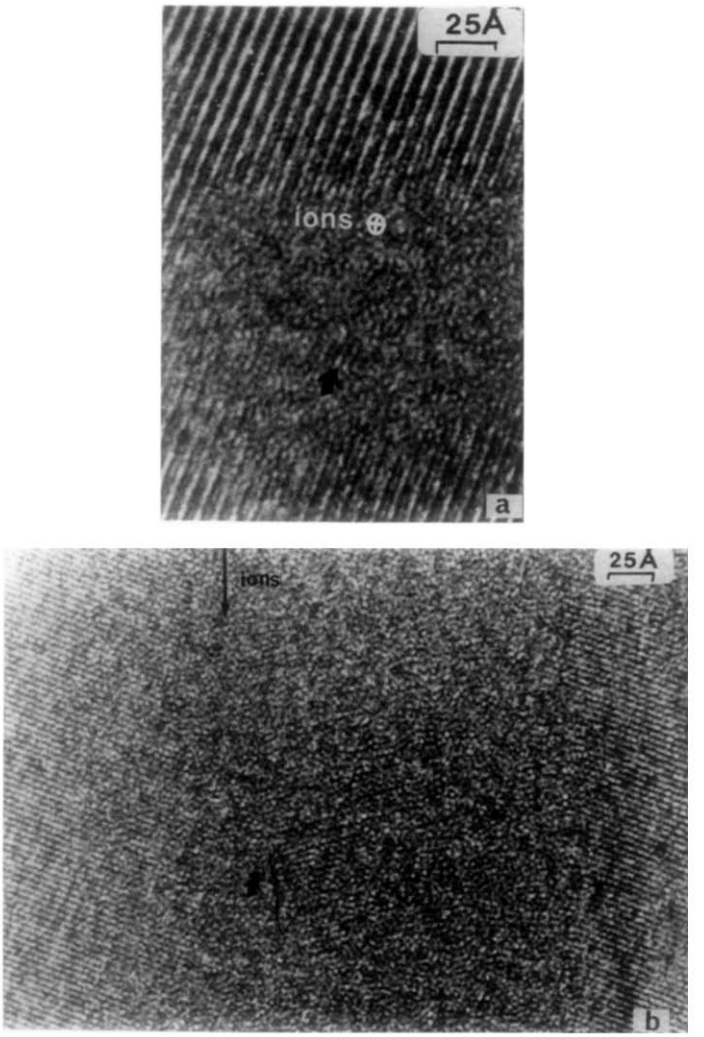

FIG. 4. High-resolution images of a latent track showing pseudocrystallized microdomains (marked with arrows) in the amorphous parts (a) in a plane normal to the ion beam and (b) parallel to the ion beam.

Moreover, the existence of small unperturbed islands 20 Å wide and showing the same zone axis as that of the unirradiated matrix (Fig. 3) cannot be solely understood on the basis of the ion explosion spike theory.

Additional effects implying the electronic thermal spike concept (*19*) have then to be considered to explain such particular features. Although the existence of thermal spike effects is still being discarded for low energy ions, it has been reported to occur in semiconductors for bombardment with 250 keV heavy ions (*20*) and in insulators for high energy sputtering experiments (*21*). Important thermal effects of fission spikes have also been postulated to explain the effects of fission-induced resolution from fission gas bubbles in ceramic nuclear fuels (*22*). They are still considered (*23*) to explain the contribution of the energy deposited by electronic collisions in the amorphization process of $Pd_{80}Si_{20}$ alloy irradiated by fission fragments of U^{235}.

Accounting for the high value of the electronic stopping power involved in the GeV energy range for xenon ions (Se $\geq$20 MeV/μm) and the probably low value of the thermal conductivity which can be expected for $Bi_2Fe_4O_9$, overheated zones may exist in the wake of the incoming ion leading to local melting of the target. As a result, the lattice image to be expected would be that of a cylinder with a strong contrast marking a sharp boundary between an external region which never reaches temperature higher than T_m and an internal region which at some instant is heated above T_m. The effect is also reflected, as described previously (*12*), in the ED patterns which show no disturbance of the diffraction spots characteristic of the remaining crystalline part of the sample. The behavior of $Bi_2Fe_4O_9$ to heavy ion impact can thus be regarded as agreeing with the thermal spike model of Naguib and Kelly (*24*). It leads us to assume that the shape of the incident ion paths corresponds exactly to the geometrical outline of the track added: a schematic drawing of such an overlapping of tracks observed in some portions of the HREM images is shown in Fig. 3.

Furthermore, as one can see in Fig. 3, the damaged portion which shows no lattice resolution, owing to the latent track overlaps, presents from place to place a granulometry which is no more aleatory and this occurs no matter what the crystal orientation and objective aperture may be. Such domains have been marked with arrows in Fig. 3 and reported for other HREM observations in Figs. 4a and 4b. These domains form regions which are about 25–30 Å long and less than 10 Å wide. The optical diffractograms of different areas showing such contrast have been registered, using a laser beam. They exhibit scattering spots of Debye rings which correspond to 2.9- and 3.1-Å reticular spacings. As a result, it may be postulated that microcrystallites have developed in the exposed region accounting for the thermal annealing track effects or stoichiometry changes as discussed elsewhere (*24*).

Acknowledgments

The irradiations were carried out with the collaboration of CIRIL. The authors thank J. Dural and J. M. Ramillon for their technical assistance and J. C. Jousset and M. Toulemonde for helpful discussions.

References

1. R. L. Fleischer, P. B. Price, and R. M. Walker, *J. Appl. Phys.* **36,** 3645 (1965).
2. R. L. Fleischer, P. B. Price, and R. M. Walker, "Nuclear Tracks in Solids: Principles and Applications," Univ. of California Press, Berkeley/London (1975).
3. P. Hansen, H. Heitmann, and P. H. Smit, *Phys. Rev. B* **26,** 3539 (1982).
4. H. Heitmann and P. Hansen, *J. Appl. Phys.* **53,** 7321 (1982).
5. K. Yada, T. Tanji, and I. Sunagawa, *Phys. Chem. Miner.* **7,** 47 (1981).

6. G. BONFIGLIOLI, A. FERRO, AND A. MOJONI, *J. Appl. Phys.* **32,** 2499 (1961).
7. P. B. PRICE AND R. M. WALKER, *J. Appl. Phys.* **33,** 3400 (1962).
8. L. T. CHADDERTON AND MC. C. TORRENS, "Fission Damage in Crystals," Methuen, London (1969).
9. M. P. A. VIEGERS, *Electron Microsc.* **2,** 187 (1982).
10. G. FUCHS, D. GROULT, M. HERVIEU, N. NGUYEN, F. STUDER, M. TOULEMONDE, AND B. RAVEAU, "Proceedings of the Third European Conference on Solid State Chemistry, Regensburg" (1986).
11. G. FUCHS, F. STUDER, E. BALANZAT, D. GROULT, M. TOULEMONDE, AND J. C. JOUSSET, *Europhys. Lett.* **3,** 327 (1987).
12. D. GROULT, M. HERVIEU, N. NGUYEN, AND B. RAVEAU, *J. Solid State Chem.* **76,** 248 (1988).
13. N. NIIZEKI AND M. WACHI, *Z. Kristallogr.* **127,** 173 (1968).
14. D. GROULT, M. HERVIEU, N. NGUYEN, B. RAVEAU, G. FUCHS, AND E. BALANZAT, *Radiat. Eff.* **90,** 191 (1985).
15. E. BALANZAT, G. FUCHS, D. GROULT, M. HERVIEU, J. C. JOUSSET, N. NGUYEN, B. RAVEAU, F. STUDER, AND M. TOULEMONDE, *Nouv. GANIL* **19,** 25 (1987).
16. M. TOULEMONDE AND F. STUDER, *Philos. Mag.*, in press (1988).
17. F. STUDER, D. GROULT, N. NGUYEN, AND M. TOULEMONDE, *Nucl. Instrum. Methods B* **20,** 856 (1987).
18. M. TOULEMONDE, G. FUCHS, N. NGUYEN, F. STUDER, AND D. GROULT, *Phys. Rev. B* **35,** 6560 (1987).
19. D. V. MORGAN AND D. VAN VLIET, *Contemp. Phys.* **11,** 173 (1970).
20. D. A. THOMPSON AND R. S. WALKER, *Radiat. Eff.* **36,** 91 (1978).
21. L. E. SIEBERLING, J. E. GRIFFITH, AND T. A. TOMBRELLO, *Radiat. Eff.* **52,** 201 (1980).
22. A. BLANK AND HJ. MATZKE, *Radiat. Eff.* **17,** 57 (1973).
23. D. LESIEUR, CEA Report R-4502 (1973).
24. H. M. NAGUIB AND R. KELLY, *Radiat. Eff.* **25,** 1 and 79 (1975).